

PREPARED FOR SUBMISSION TO JHEP

# Ramp and plateau in bulk correlators within the disk topology in JT gravity

---

**Cristiano Germani and Mickael Komendyak**

*Departament de Física Quàntica i Astrofísica and Institut de Ciències del Cosmos,  
Universitat de Barcelona, Martí i Franquès 1, 08028 Barcelona, Spain*

*E-mail:* [germani@icc.ub.edu](mailto:germani@icc.ub.edu), [komendyak@icc.ub.edu](mailto:komendyak@icc.ub.edu)

**ABSTRACT:** We show that the solution of the information paradox in Jackiw–Teitelboim gravity — manifested as a linear growth (ramp) followed by saturation (plateau) of matter correlators after an initial decay — is fully encoded in the next-to-leading-order steepest-descent approximation of the gravitational path integral. The correlators exhibiting this ramp–plateau behavior are those entangling the two sides of the eternal black hole, while those on the same side only show an exponential decay. This seems to imply that the information flows across the separate universes that are causally disconnected by the black hole horizon. Finally, we show that the dip-time, defined as the minimum of the correlator, grows inversely with the black hole temperature, as predicted by the holographic dual theory.

---

## Contents

<b>1</b>	<b>Introduction</b>	<b>2</b>
<b>2</b>	<b>JT Gravity</b>	<b>3</b>
2.1	Metric solutions	3
2.2	Schwarzian dynamics	5
<b>3</b>	<b>Scalar Correlators in JT Gravity</b>	<b>6</b>
3.1	Tree-Level Correlators	7
3.2	Gravity Correlators	7
3.3	Perturbative Expansion	8
<b>4</b>	<b>Results</b>	<b>9</b>
4.1	Bulk Correlators	10
4.2	Boundary Correlators: relation to AdS/CFT	11
<b>5</b>	<b>Conclusion</b>	<b>14</b>

---

## 1 Introduction

Black holes are known to radiate. Hawking’s seminal computation [1, 2] shows that an evaporating black hole emits an almost thermal spectrum characterized only by its macroscopic parameters (mass, charge, angular momentum). If this conclusion is extrapolated to the endpoint of evaporation, one is led to the conclusion that pure states evolve into mixed states, apparently violating unitarity and threatening the foundations of quantum mechanics. This conflict is commonly referred to as the black hole information paradox [3, 4].

One might hope that the missing information is merely hidden behind the event horizon, inaccessible to an exterior observer until the very final stages of evaporation. Page famously argued, however, that if black hole evaporation is unitary, the entanglement entropy of the Hawking radiation must begin to decrease long before the black hole shrinks to Planckian size [4, 5]. The corresponding Page time typically occurs when roughly half of the initial Bekenstein–Hawking entropy has been radiated away, at which point the black hole is still semiclassical and large. The unavoidable conclusion is that the standard Hawking calculation — firmly rooted in semiclassical gravity — must already miss an essential ingredient well before curvatures become extreme.

Confronted with this puzzle, it is natural to seek gravitational models where quantum effects are tractable and information flow can be analyzed exactly. Jackiw–Teitelboim (JT) [6, 7] gravity — two-dimensional dilaton gravity with a negative cosmological constant — has emerged as a particularly fruitful setting. Classically, it is simple: the metric has constant negative curvature and the dilaton carries the nontrivial gravitational degree of freedom. Quantum mechanically, it is nontrivial: the theory admits black holes with finite entropy and a well-defined Hamiltonian description of boundary dynamics governed by the Schwarzian action [8–10]. Moreover, JT gravity is conjectured to be the gravitational dual of the universal low-energy limit of Sachdev–Ye–Kitaev (SYK)-like models (from now on simply SYK theory) [11, 12]. This corresponds to a large number of interacting Majorana fermions at low energies (with respect to the coupling constants), see e.g. [13].

In SYK, the disorder-averaged two-point correlation functions display the characteristic dip–ramp–plateau pattern of discrete chaotic systems [12], and are governed at low energies by the Schwarzian action. This Schwarzian theory is precisely the boundary action of Jackiw–Teitelboim gravity, so the infrared dynamics of SYK provide a concrete dual description of nearly-AdS<sub>2</sub> dilaton gravity, where the same dip–ramp–plateau structure is expected to appear in bulk correlators [12, 14]. After an initial decay (“slope”) and a minimum (“dip”), the SYK correlators grow linearly (“ramp”). In chaotic systems, this growth is governed by two-level correlations between pairs of nearby energy levels, as described by random-matrix theory [15]. At late times, the disorder-averaged correlators saturate to a constant value (“plateau”) determined by the diagonal matrix elements of the operator [12].

In the bulk JT-gravity description, recent efforts to reproduce the ramp in the boundary correlators incorporate connected wormhole topologies into the gravitational path integral [14, 16–20]. The leading connected contribution arises from the so-called double-

trumpet Euclidean wormhole [19], which produces the linear ramp, while the plateau is believed to stem from genuinely non-perturbative effects in Newton’s constant [21, 22]. In this approach however, first the action must be modified by the introduction of a topological term tailor-made in order to reproduce the expected behaviors of correlators and, second, while the sum over topologies can be defined at the boundary, it is not clear what this topological sum would correspond to for bulk correlators<sup>1</sup>.

Following the philosophy of [23], in contrast to previous approaches, we work entirely within the disk topology for bulk correlators and show that the dip–ramp–plateau structure arises directly from the perturbative expansion of the vacuum Hadamard function evaluated across two maximally entangled black hole exteriors. At leading order, the correlator exhibits pure exponential decay. However, at the next perturbative order in the gravity coupling constant, it transitions into a linear growth and ultimately saturates at a constant plateau. Thus the black hole information encoded in the Hadamard function emerges once the leading order in the steepest descent expansion of the gravitational path integral becomes of the order of the first subleading correction. Crucially, this calculation relies solely on the main Lorentzian saddle — the black hole background itself.

## 2 JT Gravity

Jackiw–Teitelboim gravity is a two-dimensional model of dilaton gravity [6, 7, 19] defined by a bulk action involving the product of the dilaton scalar field  $\Phi$  and the Ricci scalar  $R$ , supplemented by the Gibbons-Hawking-York (GHY) boundary term. To focus on 2d Anti-de Sitter space ( $\text{AdS}_2$ ), we set  $\Lambda = -\frac{1}{L^2}$  and work in units where the  $\text{AdS}_2$  length is set to  $L = 1$ :

$$S_{\text{JT}}[g, \Phi] = \frac{1}{16\pi G_N} \left( \int_{\mathcal{M}} \Phi(R + 2)\sqrt{-g} dx^2 + 2 \oint_{\partial\mathcal{M}} \Phi|_{\partial} (K - 1)\sqrt{-h} dx \right). \quad (2.1)$$

### 2.1 Metric solutions

In two dimensions, the Ricci scalar  $R$  fully determines the local geometry since the Riemann tensor has only one component. Thus, varying eq.(2.1) with respect to  $\Phi$  fixes the background manifold to be locally  $\text{AdS}_2$  through  $R = -2$ . This determines the metric up to coordinate transformations.

In global coordinates, the  $\text{AdS}_2$  metric takes the form:

$$ds^2 = \frac{1}{\cos^2(z_G)} (-dt_G^2 + dz_G^2) = -\frac{1}{\cos^2(\frac{1}{2}(u_G - v_G))} du_G dv_G, \quad (2.2)$$

where  $z_G \in [0, \frac{\pi}{2}]$ ,  $t_G \in \mathbb{R}$ , and the lightcone coordinates are defined as  $u_G = t_G + z_G$  and  $v_G = t_G - z_G$ . These coordinates cover the maximal extension of the  $\text{AdS}_2$  manifold.

---

<sup>1</sup>CG thanks Vijay Balasubramanian for pointing this out.

One can get to the Poincaré patch through the transformations  $u_G = 2 \tan^{-1}(u_P) - \frac{\pi}{2}$ , and  $v_G = 2 \tan^{-1}(v_P) + \frac{\pi}{2}$ :

$$ds^2 = \frac{1}{z_P^2}(-dt_P^2 + dz_P^2) = -\frac{4}{(u_P - v_P)^2} du_P dv_P, \quad (2.3)$$

where  $z_P \in (0, \infty)$ , and  $t_P \in \mathbb{R}$ . This patch covers only a region inside the global manifold. The Poincaré time  $t_P$  does not correspond to the global time  $t_G$  and therefore one expects the Poincaré vacuum to be different from the global vacuum. However, as was shown in [24, 25] this is not the case and both vacua are in fact equivalent.

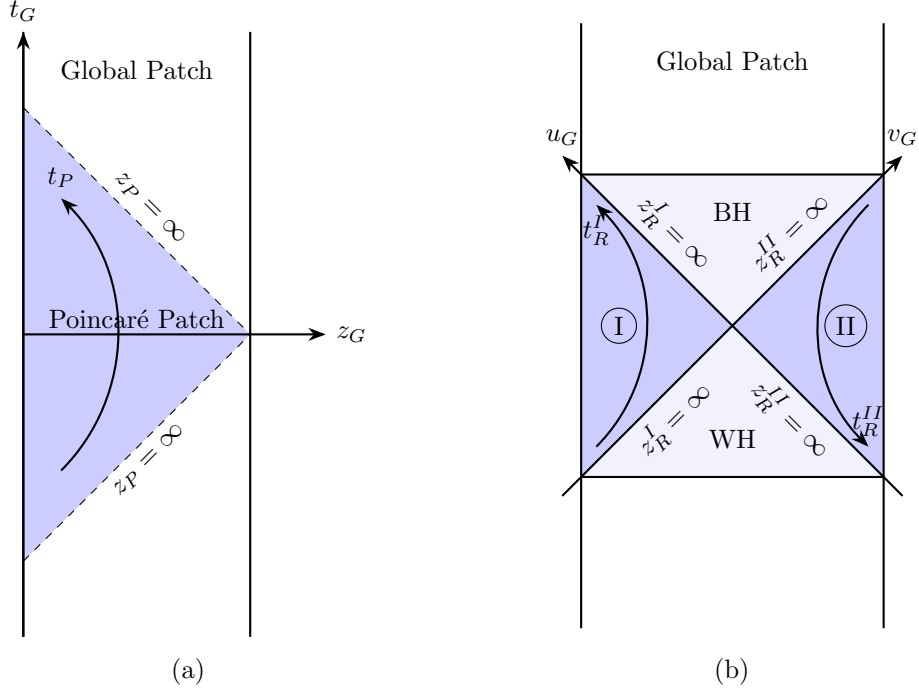


**Figure 1:** Three coordinate systems on  $AdS_2$ : (a) Global and Poincaré patches. (b) Global and Schwarzschild patches.

Furthermore, one can introduce Rindler (or equivalently Schwarzschild) coordinates to describe two black hole exterior patches in the global  $AdS_2$  manifold:

$$\text{Patch } \textcircled{I} \begin{cases} u_G = 2 \tan^{-1} \left[ \frac{\beta}{\pi} \tanh \left( \frac{\pi}{\beta} u_R^I \right) \right] - \frac{\pi}{2}, \\ v_G = 2 \tan^{-1} \left[ \frac{\beta}{\pi} \tanh \left( \frac{\pi}{\beta} v_R^I \right) \right] + \frac{\pi}{2}, \end{cases} \quad (2.4)$$

$$\text{Patch } \textcircled{II} \begin{cases} u_G = -2 \tan^{-1} \left[ \frac{\beta}{\pi} \tanh \left( \frac{\pi}{\beta} u_R^{II} \right) \right] + \frac{\pi}{2}, \\ v_G = -2 \tan^{-1} \left[ \frac{\beta}{\pi} \tanh \left( \frac{\pi}{\beta} v_R^{II} \right) \right] - \frac{\pi}{2}. \end{cases} \quad (2.5)$$

The constant  $\beta$  is related to the acceleration of an observer at fixed  $z_R$  (or, equivalently to the "black hole" mass) and quantum mechanically corresponds to the inverse horizon temperature [26].

The resulting Rindler metric takes the form:

$$ds^2 = \left(\frac{2\pi}{\beta}\right)^2 \frac{1}{\sinh^2\left(\frac{2\pi}{\beta}z_R\right)} (-dt_R^2 + dz_R^2) = -\left(\frac{2\pi}{\beta}\right)^2 \frac{1}{\sinh^2\left(\frac{\pi}{\beta}(u_R - v_R)\right)} du_R dv_R, \quad (2.6)$$

where  $z_R \in (0, \infty)$ , and  $t_R \in \mathbb{R}$  in both patches, each of which is causally disconnected from the other by an event horizon at  $z_R^I, z_R^{II} = \infty$ .

Using the radial coordinate  $r = r_h \coth(r_h z_R)$ , one can also rewrite this metric in the Schwarzschild form:

$$ds^2 = -f(r) dt_R^2 + \frac{dr^2}{f(r)}, \quad (2.7)$$

where  $r \in (r_h, \infty)$ ,  $f(r) = r^2 - r_h^2$ , and the horizon is now located at  $r_h = \frac{2\pi}{\beta}$ .

Each of the patches in Fig.1 (b) and eqs.(2.4) and (2.5) possesses its own asymptotic boundary and its own timelike Killing vector generating time evolution  $t_R$  within that patch. The two exterior regions are smoothly connected by an Einstein–Rosen bridge, forming a smooth but non-traversable wormhole that connects the asymptotic boundaries at one instant of global time. In the holographic dual description, the two asymptotic boundaries correspond to decoupled boundary CFTs [27]. Quantum mechanically, the two-sided eternal AdS geometry is realized by a thermofield-double (TFD) state of the two boundary theories [28]; the entanglement between them purifies each boundary thermal density matrix and is manifested in the bulk as a connected Einstein–Rosen bridge [29].

## 2.2 Schwarzsian dynamics

Putting the bulk term of eq.(2.1) on shell selects the background manifold and reduces the JT action to the GHY boundary term [9, 10, 13]. Performing the gravitational path integral is then equivalent to summing over  $\text{AdS}_2$  manifolds with different boundaries. To study the dynamics of these boundaries we cut the manifold along a constant value of the dilaton in an arbitrary coordinate system.

Varying eq.(2.1) with respect to the metric results in the vacuum equations of motion for the dilaton field:

$$\nabla_\mu \nabla_\nu \Phi - g_{\mu\nu} \nabla^2 \Phi + g_{\mu\nu} \Phi = 0. \quad (2.8)$$

Solving eq.(2.8) in Poincaré coordinates, eq.(2.3), one obtains a divergent dilaton profile [13]:

$$\Phi(t_P, z_P) = \frac{A + Bt_P + C(t_P^2 + z_P^2)}{z_P}, \quad (2.9)$$

where  $A$ ,  $B$ , and  $C$  are arbitrary parameters of the theory. Clearly, the dilaton field diverges at the boundary  $z_P = 0$ . However, the theory can be regulated by introducing a near-boundary cutoff [10, 13].

The gravitational path integral is defined for metrics which are asymptotically  $\text{AdS}_2$ :

$$ds^2 = \frac{1}{z^2}(-dt^2 + dz^2) + \mathcal{O}(z^{-1}) \quad \text{as } z \rightarrow 0, \quad (2.10)$$

while imposing fixed divergent asymptotics for the dilaton field:

$$\Phi = \frac{a}{2z} + \mathcal{O}(z) \quad \text{as } z \rightarrow 0, \quad (2.11)$$

where  $a$  is the regularised value of the dilaton. Performing an arbitrary coordinate transformation  $u_P(u, v)$ ,  $v_P(u, v)$ , the first boundary condition, eq.(2.10), forces  $\partial_u v_P = \partial_v u_P = 0$  and  $u_P(u, v) = v_P(u, v)$  at leading order in  $z$  as  $z \rightarrow 0$ :

$$\begin{cases} u_P(u) = F(u) + \mathcal{O}(z), \\ v_P(v) = F(v) + \mathcal{O}(z). \end{cases} \quad (2.12)$$

In the Poincaré patch, the boundary  $z = \epsilon$  is therefore parameterized by:

$$\begin{cases} t_P(t) = \frac{1}{2}(u_P + v_P) = F(t) + \mathcal{O}(\epsilon), \\ z_P(t) = \frac{1}{2}(u_P - v_P) = \epsilon F'(t) + \mathcal{O}(\epsilon^2), \end{cases} \quad (2.13)$$

has induced metric  $\sqrt{-h} = \frac{1}{\epsilon} + \mathcal{O}(\epsilon)$  and extrinsic curvature trace:

$$K = 1 + \epsilon^2 \{F(t), t\} + \mathcal{O}(\epsilon^4), \quad (2.14)$$

where the Schwarzian derivative is defined as:

$$\{F, t\} := \frac{F'''(t)}{F'(t)} - \frac{3}{2} \left( \frac{F''(t)}{F'(t)} \right)^2. \quad (2.15)$$

The second boundary condition, eq.(2.11), forces the regulated value of the dilaton at this boundary to be  $\Phi|_{\partial} = \frac{a}{2\epsilon} + \mathcal{O}(\epsilon)$ .

Finally, the bulk gravitational action, eq.(2.1), simplifies to the Schwarzian action governing the dynamics of the boundary:

$$S_{\text{JT}}[g, \Phi] = \frac{1}{8\pi G_N} \int_{\partial\mathcal{M}} \Phi|_{\partial} (K - 1) \sqrt{-h} dt = \frac{a}{16\pi G_N} \int \{F(t), t\} dt \quad (2.16)$$

### 3 Scalar Correlators in JT Gravity

We are interested in calculating the vacuum correlation of a massless scalar field  $\phi$ , including gravitational fluctuations. For simplicity, we assume a field decoupled from the dilaton, therefore ignoring backreaction.

### 3.1 Tree-Level Correlators

The  $\text{AdS}_2$  vacuum is fully specified by the two-point function  $G_{12} = \langle \phi(x_1) \phi(x_2) \rangle$ . In Lorentzian spacetimes there exist various Green functions; we focus on the Hadamard function:

$$H_{12} = \langle \{ \phi(x_1), \phi(x_2) \} \rangle, \quad (3.1)$$

which is related to the Feynman propagator  $G_{12}^F = i \langle T \phi(x_1) \phi(x_2) \rangle$  by  $H_{12} = 2 \text{Im} G_{12}^F$ .

The fixed background Hadamard function of the global  $\text{AdS}_2$  vacuum is known to be [24]:

$$H_{12} = -\frac{1}{2\pi} \ln \left| \frac{\cos(t_G - t'_G) - \cos(z_G - z'_G)}{\cos(t_G - t'_G) + \cos(z_G + z'_G)} \right|. \quad (3.2)$$

One can express this function in Rindler coordinates, eq.(2.4) and eq.(2.5), to obtain a thermal vacuum in either of the two BH exteriors. To evaluate the correlator in only one patch, we choose the coordinates corresponding to that patch. For example in the left exterior:

$$H_{12}^{LL} = -\frac{1}{2\pi} \ln \left| \frac{\sinh \frac{\pi}{\beta} (u_{R,1}^I - u_{R,2}^I) \sinh \frac{\pi}{\beta} (v_{R,1}^I - v_{R,2}^I)}{\sinh \frac{\pi}{\beta} (v_{R,1}^I - u_{R,2}^I) \sinh \frac{\pi}{\beta} (u_{R,1}^I - v_{R,2}^I)} \right|. \quad (3.3)$$

Furthermore, one can also investigate the global vacuum correlation across both BH patches:

$$H_{12}^{LR} = -\frac{1}{2\pi} \ln \left| \frac{\cosh \frac{\pi}{\beta} (u_{R,1}^I + v_{R,2}^{II}) \cosh \frac{\pi}{\beta} (v_{R,1}^I + u_{R,2}^{II})}{\cosh \frac{\pi}{\beta} (v_{R,1}^I + v_{R,2}^{II}) \cosh \frac{\pi}{\beta} (u_{R,1}^I + u_{R,2}^{II})} \right|. \quad (3.4)$$

### 3.2 Gravity Correlators

In the Rindler patch the boundary reparametrization is given by  $F(t_R) = \tanh \frac{\pi}{\beta} f(t_R)$  at leading order as  $z_R \rightarrow 0$ , where  $f(t_R)$  is a function that satisfies:

$$f(t_R + i\beta) = f(t_R) + i\beta, \quad f'(t_R) \geq 0. \quad (3.5)$$

The first relation enforces that  $f$  wraps around the Euclidean thermal circle once for each period  $\beta$  in  $\tau = it_R$ . The second requirement guarantees  $f$  is monotone and thus orientation preserving. These properties, after Wick rotation, identify  $f$  as an element of the diffeomorphism group of the circle,  $\text{Diff}(\mathbb{S}^1)$ , and justify interpreting it as a boundary time reparametrization.

Since the JT integral eq.(2.1) always reduces to a boundary term after the background manifold is selected, integrating the Hadamard function over metrics is equivalent to an integration over the boundary function  $f(t_R)$  [10, 13, 16, 18–20]:

$$\langle H_{12} \rangle = \text{Re} \left( \frac{\int H_{12}[g] e^{iS_{JT}[g, \Phi]} \mathcal{D}g \mathcal{D}\Phi}{\int e^{iS_{JT}[g, \Phi]} \mathcal{D}g \mathcal{D}\Phi} \right) = \text{Re} \left( \frac{\int H_{12}[f] e^{iS_{JT}[f]} d\mu[f]}{Z(\lambda)} \right), \quad (3.6)$$



where  $Z(\lambda) = \int e^{iS_{JT}[f]} d\mu[f]$  is the vacuum normalization,  $H_{12}[f]$  is the bulk Hadamard function evaluated on the metric parametrized by  $f$ , and  $d\mu[f]$  is the measure of integration over the symplectic manifold  $\text{Diff}(\mathbb{S}^1)/SL(2, \mathbb{R})$  [30].

After Wick rotating the boundary action  $iS_{JT} \rightarrow I$ , rescaling the boundary circle to  $\hat{\tau} = \frac{2\pi}{\beta}\tau$  and  $\hat{f}(\hat{\tau}) = \frac{2\pi}{\beta}f(\tau)$ , and evaluating the Pfaffian measure  $d\mu[\hat{f}]$  in terms of a Grassmann field  $\psi$  [16, 30], the bulk quantum gravity correlator evaluates to:

$$\langle H_{12} \rangle = \text{Re} \left( \frac{\int H_{12}[\hat{f}] e^{-\frac{1}{2}I[\hat{f}, \psi]} \mathcal{D}\hat{f} \mathcal{D}\psi}{Z(\lambda)} \right), \quad (3.7)$$

where the Euclidean action is a functional of the boundary functions  $\hat{f}(\hat{\tau})$  and  $\psi(\hat{\tau})$ :

$$I[\hat{f}, \psi] = \int_0^{2\pi} \frac{\ddot{\hat{f}}^2}{\lambda^2 \dot{\hat{f}}^2} - \frac{\dot{\hat{f}}^2}{\lambda^2} + \frac{\ddot{\psi}\dot{\psi}}{\dot{\hat{f}}^2} - \dot{\psi}\psi \, d\hat{\tau}, \quad (3.8)$$

with  $\lambda^2 = \frac{8G_N\beta}{a}$ .

In the following we shall assume that the gravity coupling constant  $\lambda \ll 1$  and fixed. This will justify a perturbative expansion in  $\lambda$ .

### 3.3 Perturbative Expansion

The saddle of the action eq.(2.16), with the periodicity requirement eq.(3.5), is  $\hat{f}_s(\hat{\tau}) = \hat{\tau}$  [10, 13, 19]. At the saddle, it is easy to see that all the  $\langle H_{12} \rangle$  exponentially decay in time implying an information paradox. From the point of view of the gravitational path integral, this simply implies that, at large times  $H_{12}(\hat{f}_s) \rightarrow 0$ . In this case then, unless all derivatives  $\left. \frac{d^n H_{12}}{d\hat{f}^n} \right|_{\hat{f}=\hat{f}_s}$  vanish, the steepest descent approximation requires to go next to leading order in the expansion parameter  $\lambda$  until the  $n$ -th derivative would be finite. This was the approach adopted in [23]. If at least one of the correlators  $\langle H_{12} \rangle$  would not decay exponentially to zero, the paradox would not hold and the information would be canalized on these correlators [27].

For small  $\lambda$ , one can use the method of stationary phase to asymptotically expand the functional part of the integral eq.(3.7) in powers of  $\lambda$  around the saddle point  $\hat{f}_s$ . In other words, we shall consider  $\hat{f}(\hat{\tau}) = \hat{\tau} + \lambda\gamma(\hat{\tau}) + \dots$  at leading order in  $\lambda$ . By using the map of boundary correlators versus bulk correlators introduced in [20], in [23] it was found a linear ramp after an exponential decay for  $\langle H_{12}^{LL} \rangle$  at quadratic order in  $\lambda$ . After a close inspection, a growth is encoded already inside the  $\gamma$ 's boundary correlators, in particular in  $\langle \gamma(\hat{\tau}_1) \dot{\gamma}(\hat{\tau}_2) \rangle$ . However, the result of the linear growth of  $\langle H_{12}^{LL} \rangle$  was at odds with the calculation done in [8]. The reason of this mismatch, we found, was rooted in a sign mistake in the correlator  $\langle \gamma(\hat{\tau}_1) \dot{\gamma}(\hat{\tau}_2) \rangle$  used in [23] (c.f. [31]) that, interestingly, by correcting it, would sum to zero the linear growth of  $\langle H_{12}^{LL} \rangle$  at  $\lambda^2$ . In other words, the replacement  $\langle \gamma(\hat{\tau}_1) \dot{\gamma}(\hat{\tau}_2) \rangle \rightarrow -\langle \gamma(\hat{\tau}_1) \dot{\gamma}(\hat{\tau}_2) \rangle$  was responsible for the seeming resolution of the information paradox in JT gravity. This mirror symmetry is naively related to a time reverse of the derivative of the two point correlation function. Indeed, as we are going to show, the linear

ramp is now obtained in the correlator  $H_{12}^{LR}$  connecting the two black hole exteriors of the maximally extended geometry (2.6).

Expanding the action, eq.(3.8), in powers of  $\lambda$ , we have:

$$I[\hat{\tau} + \lambda\gamma(\hat{\tau}), \psi] = -\frac{2\pi}{\lambda^2} + I_0[\gamma, \psi] + \sum_{k=1}^{\infty} \lambda^k I_k[\gamma, \psi], \quad (3.9)$$

where:

$$I_0[\gamma, \psi] = \int_0^{2\pi} \ddot{\gamma}^2 - \dot{\gamma}^2 + \ddot{\psi}\dot{\psi} - \dot{\psi}\dot{\psi} d\hat{\tau}, \quad (3.10)$$

and

$$I_k[\gamma, \psi] = (-1)^k (k+1) \int_0^{2\pi} \dot{\gamma}^k (\ddot{\gamma}^2 + \ddot{\psi}\dot{\psi}) d\hat{\tau}. \quad (3.11)$$

Similarly, one can expand the bulk correlator  $H_{12}[\hat{\tau} + \lambda\gamma] = \sum_0^{\infty} \lambda^k H_k[\gamma]$ , to obtain the full perturbative expansion:

$$\langle H_{12} \rangle = \text{Re} \left( \frac{\int \left( \sum_{k=0}^{\infty} \lambda^k H_k \right) e^{\frac{\pi}{\lambda^2}} e^{-\frac{1}{2} I_0} e^{-\frac{1}{2} \sum_{k=1}^{\infty} \lambda^k I_k} \mathcal{D}\gamma}{Z_{1-loop}(\lambda)} \right) = \sum_{k=0}^{\infty} \lambda^k \langle \Gamma_n \rangle,$$

$$\begin{aligned} \text{where: } \Gamma_0 &= H_0, \\ \Gamma_1 &= \text{Re}(H_1 + H_0 I_1), \\ \Gamma_2 &= \text{Re}(H_2 + H_1 I_1 + \frac{1}{2}(I_1^2 - 3I_2)), \\ &\vdots \end{aligned} \quad (3.12)$$

and where we used the fact that the Schwarzian theory is one-loop exact [30]. For each order in  $\lambda$ ,  $\langle \Gamma_n[\gamma, \psi] \rangle$  is a Gaussian integral involving correlations of the perturbation [32]:

$$\begin{aligned} \langle T\gamma(\hat{\tau}_1)\gamma(\hat{\tau}_2) \rangle &= \int \gamma(\hat{\tau}_1)\gamma(\hat{\tau}_2) e^{-I_0[\gamma]} \mathcal{D}\gamma \\ &= \frac{1}{2\pi} \left( 1 + \frac{\pi^2}{6} - \frac{1}{2}(\pi - \hat{\tau})^2 - (\pi - \hat{\tau}) \sin(\hat{\tau}) + \frac{5}{2} \cos(\hat{\tau}) \right), \end{aligned} \quad (3.13)$$

where  $\hat{\tau} = |\hat{\tau}_1 - \hat{\tau}_2|$ . All odd orders of the expansion vanish and one is left with  $\langle \Gamma_2 \rangle$  as the first quantum correction.

## 4 Results

To justify the perturbative expansion, we fix  $\lambda^2 = 0.1$ . Furthermore, we are interested in investigating the large time behavior of the gravitational path integral of the correlators in eq.(3.3) and eq.(3.4). For this we fix a bulk point  $z_{R,1} = z_{R,2} = z_R$ , and set  $t_{R,1} = 0$  and  $t_{R,2} = t_R$ . Finally, in order to compare the  $\beta$  dependence of the gravitationally dressed correlators in a coordinate invariant way, we anchor the first bulk point at  $t_P = 0$  and

$z_P = 1$ , and then find the corresponding  $z_R$ . To stay outside of the event horizon of the black hole we then require  $\beta > \pi$ .

#### 4.1 Bulk Correlators

First, let us investigate the one-sided bulk correlator. As described above, we set  $t_{R,1}^I = 0$ ,  $t_{R,2}^I = t_R$ , and  $z_{R,1}^I = z_{R,2}^I = z_R = \frac{\beta}{\pi} \arctan\left(\frac{\pi}{\beta}\right)$ . One finds that this correlator decays in time at both orders  $\lambda^0$  and  $\lambda^2$ , as can be seen directly from Fig.2 and Fig.3. This is in agreement with [8].

Specifically, taking the large time limit yields:

$$\begin{aligned}\langle \Gamma_0^{LL} \rangle &\sim -\frac{2}{\pi} e^{-\frac{2\pi}{\beta} t_R} \sinh^2\left(\frac{2\pi}{\beta} z_R\right), \quad t_R \rightarrow \infty, \\ \langle \Gamma_2^{LL} \rangle &\sim -\frac{8\pi}{\beta^2} t_R^2 e^{-\frac{2\pi}{\beta} t_R} \sinh^2\left(\frac{2\pi}{\beta} z_R\right), \quad t_R \rightarrow \infty.\end{aligned}\tag{4.1}$$

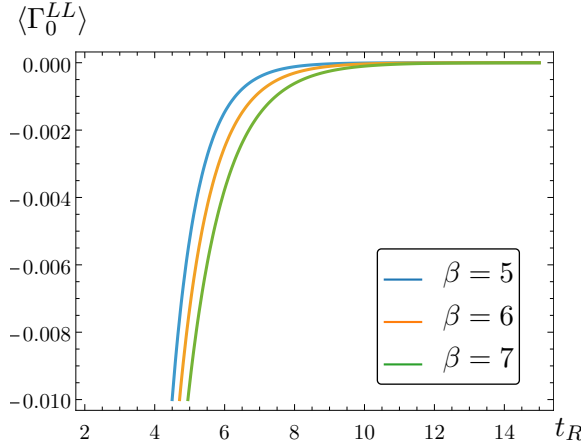


**Figure 2:** One-sided bulk saddle correlator plotted for different values of  $\beta$  and at  $z_P = 1$ .

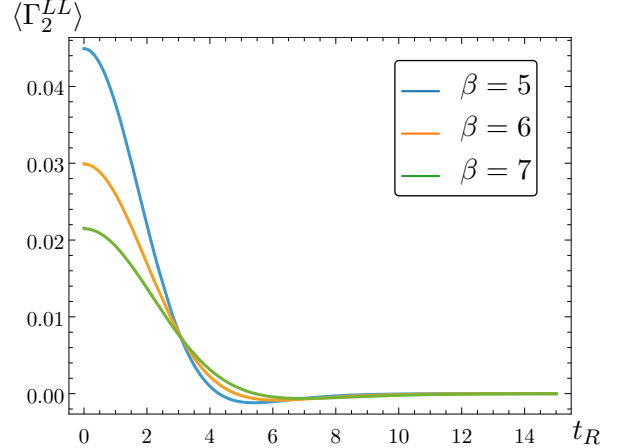


**Figure 3:** First gravitational correction to the one-sided bulk correlator plotted for different values of  $\beta$  and at  $z_P = 1$ .

This behavior reflects the suppression of correlations between bulk points on the same side of the maximally extended geometry, consistent with the presence of an event horizon. As first shown by Hawking [3], such exponential decay of correlations is the hallmark of semiclassical black hole dynamics, where the horizon leads to thermal emission and apparent information loss.

In contrast, the two-sided correlator develops a qualitatively different late-time structure. Setting  $t_{R,1}^I = 0$ ,  $t_{R,2}^{II} = t_R$ , and  $z_{R,1}^I = z_{R,2}^{II} = z_R = \frac{\beta}{\pi} \arctan\left(\frac{\pi}{\beta}\right)$ , the bulk two-sided correlator decays to zero for large time at tree level only, as shown in Fig.4. At order  $\lambda^2$  the correlator asymptotes to a negative but constant value, as seen in Fig.5.

Taking the large time limit, one obtains:

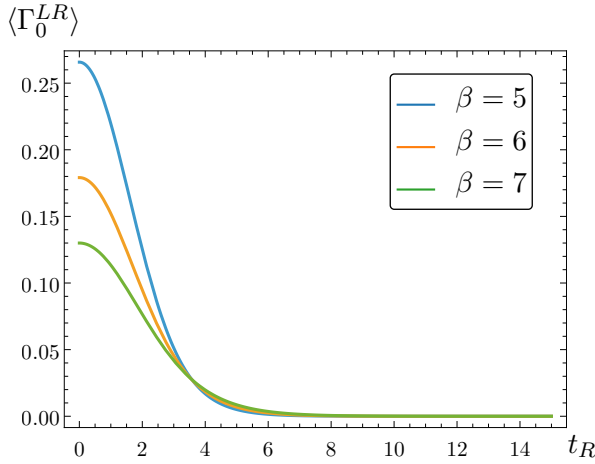


**Figure 4:** Two-sided bulk saddle correlator plotted for different values of  $\beta$  and at  $z_P = 1$ .

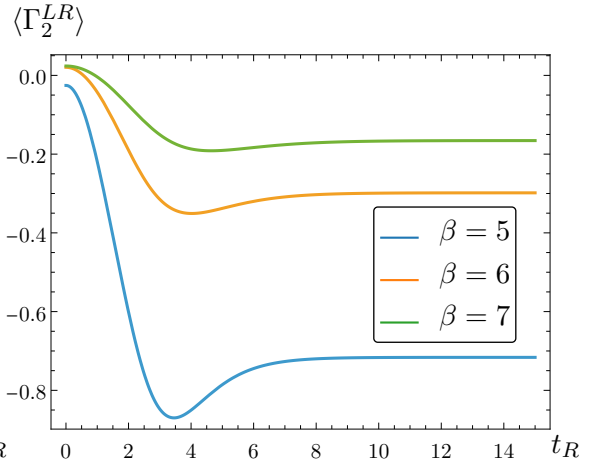


**Figure 5:** First gravitational correction to the two-sided bulk correlator plotted for different values of  $\beta$  and at  $z_P = 1$ .

$$\begin{aligned}\langle \Gamma_0^{LR} \rangle &\sim \frac{2}{\pi} e^{-\frac{2\pi}{\beta} t_R} \sinh^2 \left( \frac{2\pi}{\beta} z_R \right), \quad t_R \rightarrow \infty, \\ \langle \Gamma_2^{LR} \rangle &\sim -\frac{2z_R}{\pi\beta} \cosh \left( \frac{2\pi}{\beta} z_R \right) \sinh \left( \frac{2\pi}{\beta} z_R \right), \quad t_R \rightarrow \infty.\end{aligned}\tag{4.2}$$

Although the leading saddle contribution  $\langle \Gamma_0^{LR} \rangle$  decays exponentially with time (eq.(4.2) and Fig.4), the next to leading order correction  $\langle \Gamma_2^{LR} \rangle$  introduces a ramp that compensates the decay and drives the correlator towards a late-time constant plateau, Fig.5. This signals the restoration of non-vanishing correlations across the two exterior patches and represents the perturbative realization of information-preserving dynamics within the TFD geometry.

Adding both orders of the two-sided correlator together, the bulk gravity correlator  $\langle H_{12}^{LR} \rangle \sim \langle \Gamma_0^{LR} \rangle + \lambda^2 \langle \Gamma_2^{LR} \rangle$  exhibits the complete dip–ramp–plateau structure characteristic of chaotic systems, as can be seen on Fig.6. In this framework, the plateau emerges already at order  $\lambda^2$ , without requiring any higher-order or non-perturbative corrections, and while remaining fully within the disk topology.

Finally, defining  $t_{dip}$  as the minimum of  $\langle H_{12}^{LR} \rangle$ , one finds, after fixing  $\lambda$ , that  $t_{dip}$  exhibits a linear dependence on  $\beta$  away from the event horizon of the black hole, as can be seen in Fig.7. This is in accordance with random matrix theory [19]. Furthermore, the same plot displays the redshift of the time coordinate  $t_R$  as the horizon radius crosses the bulk point  $z_P = 1$  at  $\beta = \pi$ .

## 4.2 Boundary Correlators: relation to AdS/CFT

To obtain the boundary CFT correlators, in AdS/CFT one takes the near-boundary limit of the bulk two-point functions. For a massless scalar field in  $\text{AdS}_2$ , the scaling dimension is  $\Delta = 1$ ; hence the boundary correlators are extracted by taking the limit [33]:

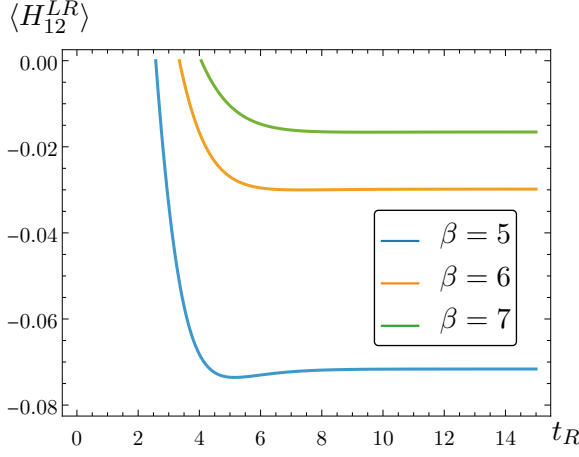


**Figure 6:** Two-sided bulk gravity correlator plotted for different values of  $\beta$ ,  $\lambda^2 = 0.1$ , and at  $z_P = 1$ .

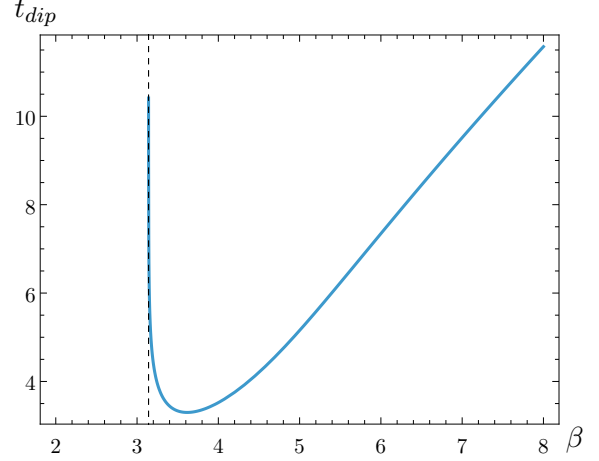


**Figure 7:** Minimum of the two-sided bulk gravity correlator plotted as a function of  $\beta$ , for  $\lambda^2 = 0.1$ , and at  $z_P = 1$ .

$$\langle \tilde{H}_{12} \rangle = \lim_{z \rightarrow 0} (z^{-2} \langle H_{12} \rangle). \quad (4.3)$$

Applying this to eq.(3.3) and eq.(3.4) results in the boundary saddle CFT correlators:

$$\begin{aligned} \tilde{H}_{12}^{LL} &= -\frac{2\pi}{\beta^2} \frac{1}{\sinh^2 \left( \frac{\pi}{\beta} (t_{R,1}^I - t_{R,2}^I) \right)}, \\ \tilde{H}_{12}^{LR} &= \frac{2\pi}{\beta^2} \frac{1}{\cosh^2 \left( \frac{\pi}{\beta} (t_{R,1}^I + t_{R,2}^I) \right)}. \end{aligned} \quad (4.4)$$

One expects the boundary correlators to retain the features of their corresponding bulk functions. Setting  $t_{R,1}^I = 0$  and  $t_{R,2}^I = t_{R,2}^{II} = t_R$ , and taking the large time limit yields:

$$\tilde{H}_{12}^{LL} \sim -\frac{8\pi}{\beta^2} e^{-\frac{2\pi}{\beta} t_R}, \quad \tilde{H}_{12}^{LR} \sim \frac{8\pi}{\beta^2} e^{-\frac{2\pi}{\beta} t_R}, \quad t_R \rightarrow \infty, \quad (4.5)$$

$$\langle \tilde{\Gamma}_2^{LL} \rangle \sim -\frac{32\pi^3}{\beta^4} t_R^2 e^{-\frac{2\pi}{\beta} t_R}, \quad \langle \tilde{\Gamma}_2^{LR} \rangle \sim -\frac{4}{\beta^2}, \quad t_R \rightarrow \infty. \quad (4.6)$$

Clearly, the one-sided correlator decays exponentially for large time at both orders  $\lambda^0$  and  $\lambda^2$ . However, the cross-boundary correlator decays exponentially at order  $\lambda^0$  only.

Plotting the full expression for the next to leading order of both correlators, one obtains the same dip-ramp-plateau features, shown in Fig.8 and Fig.9. The crucial difference is that the height of the plateau of the one-sided correlator is zero for all values of  $\beta$ , whereas the height of the plateau of the cross-boundary correlator is  $\beta$  dependent.

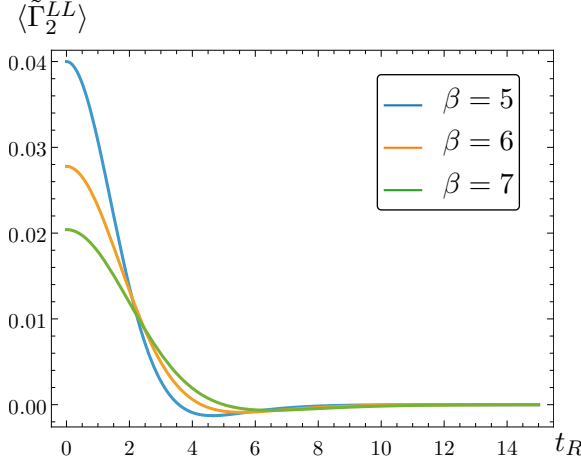


**Figure 8:** First gravitational correction to the one-sided boundary correlator plotted for different values of  $\beta$ .

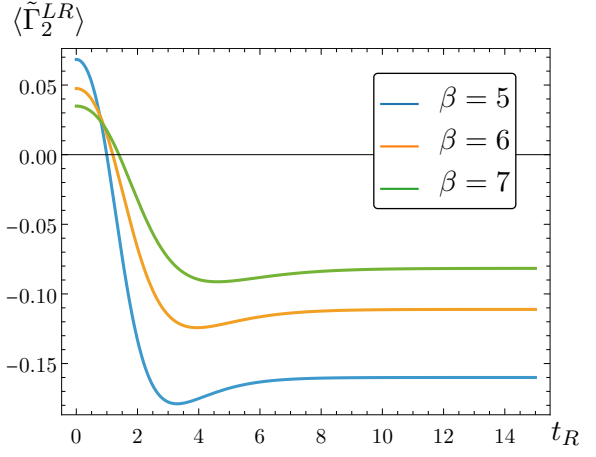


**Figure 9:** First gravitational correction to the cross-boundary correlator plotted for different values of  $\beta$ .

On the other hand, plotting both orders of the boundary gravity correlators, one clearly observes the complete dip-ramp-plateau structure emerging only for the cross-boundary correlator. As shown in Fig.10, the one-sided boundary correlator decays exponentially at all temperatures, reflecting the loss of correlations across the horizon and reproducing the expected semiclassical behavior. In contrast, Fig.11 shows the cross-boundary correlator displaying a clear dip-ramp-plateau structure whose amplitude and timescale depend on  $\beta$ . The initial dip corresponds to the semiclassical decay, while the subsequent ramp and saturation indicate the re-emergence of correlations between the two boundaries.

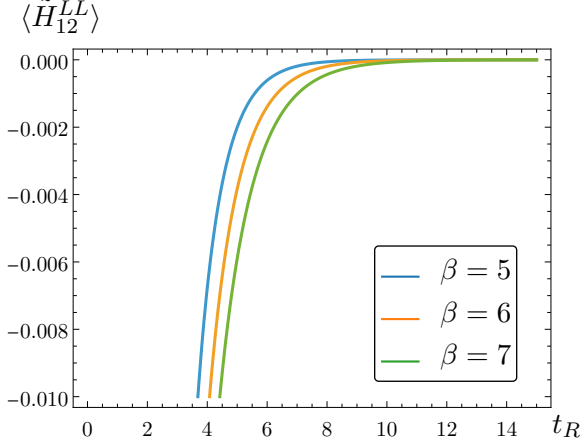


**Figure 10:** One-sided boundary gravity correlator plotted for different values of  $\beta$ .

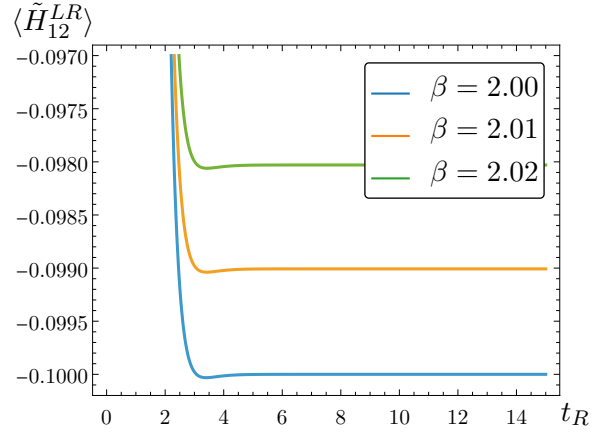


**Figure 11:** Cross-boundary gravity correlator plotted for different values of  $\beta$ .

This late-time plateau for the cross-boundary correlator realizes, within the perturbative framework, the same qualitative behavior found in the spectral form factor of the

SYK model [12, 14], signaling information-preserving dynamics consistent with holographic expectations.

Finally, now defining  $t_{dip}$  as the minimum of  $\langle \tilde{H}_{12}^{LR} \rangle$ , one finds, after fixing  $\lambda$ , that  $t_{dip} \sim \beta$ , as can be seen from Fig.12. This is in agreement with random matrix theory [19].

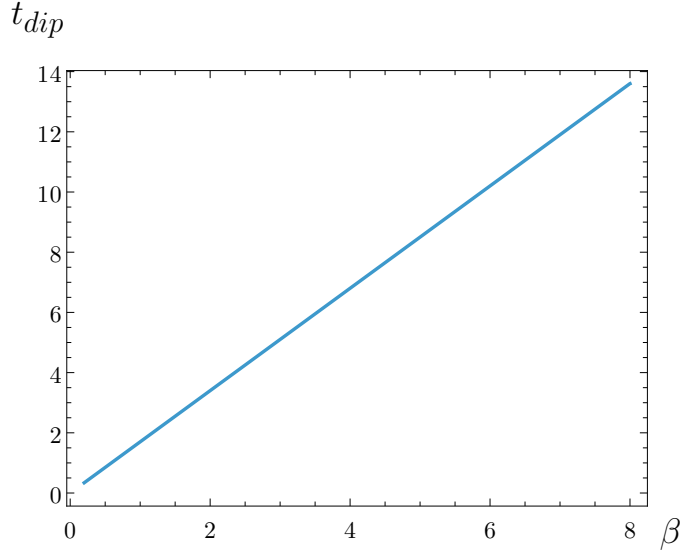


**Figure 12:** Minimum of the cross-boundary gravity correlator plotted as a function of  $\beta$  and for  $\lambda^2 = 0.1$ .

## 5 Conclusion

In this work we have shown that the characteristic dip–ramp–plateau behavior of chaotic quantum systems emerges directly from bulk correlators in Jackiw–Teitelboim gravity, without invoking topology change or non-perturbative saddles. By evaluating the gravitationally dressed Hadamard function through the next-to-leading term in the steepest-descent expansion of the Schwarzian path integral, we found that correlators evaluated in a single black hole exterior region decay exponentially at all orders considered, reproducing the semiclassical suppression. In contrast, correlators linking the two disconnected black hole exteriors undergo a transition: after their semiclassical decay, the  $\mathcal{O}(\lambda^2)$  contribution produces first a linear growth and then a saturation to a constant value. The resulting bulk and boundary correlators exhibit a complete dip–ramp–plateau structure already at this perturbative order.

These findings demonstrate that the restoration of late-time correlations—often associated with the inclusion of wormhole geometries in Euclidean formulations—arises here from the dynamics of boundary reparametrization modes around the Lorentzian black hole saddle. The location of the dip shows the expected  $\beta$ -dependence familiar from random matrix theory, while remaining entirely within the disk topology. This suggests that part of

the mechanism usually attributed to ensemble averaging or topology summation is already encoded in the perturbative gravitational response of the TFD geometry.

The analysis indicates that information flow across the two exterior regions is captured perturbatively in JT gravity and that the first quantum correction to the gravitational path integral is sufficient to restore late-time correlations. Extending these results beyond massless fields, exploring back-reaction, and identifying the precise interplay with non-perturbative corrections remain natural next steps. More broadly, our results strengthen the view that the essential features underlying the resolution of the information paradox can already be seen in controlled perturbation theory around a single, fixed saddle [23].

It might seem, however, puzzling why the holographic approach of summing over different topologies would provide the same result as ours. In the sum over topologies the weight of each configuration is related to an external parameter  $S_0 \sim 1/G_N$ , a posteriori fixed to match the dual SYK theory [19]. In particular, one would find that, apart from the linear growth of  $t_{dip}$  with respect to  $\beta$  that we also found,  $t_{dip} \propto e^{S_0}$ . In our approach, however,  $t_{dip}$  is part of the theory and related to  $\lambda$ , which we fix. Because  $S_0 \sim 1/G_N \propto 1/\lambda^2$ , decreasing  $\lambda$  should increase  $t_{dip}$ , according to the holographic dual theory, which is precisely what we found. Nevertheless, although the trend is right, one should note that neither  $S_0$  nor  $\lambda$  depend only on  $G_N$ . Thus, the exponential dependence of  $t_{dip}$  on  $S_0$  is just another way to rewrite the dependence of  $S_0$  on extra unknown parameters. This exponential dependence seems to be at the root of the holographic statement that the plateau should be related to non-perturbative physics. In our case instead, as  $t_{dip}$  (and the plateau time/magnitude) solely depends on the specifications of our system and not from any external, a posteriori, fixed parameter, the dip time (and plateau time/magnitude) is completely within reach of perturbation theory. Specifically, as the dip time is obtained as the crossing between an exponential decay and a linear growth,  $t_{dip} \sim |\ln \lambda^2|$ , implying that  $S_0 \sim \ln(|\ln(\lambda^2)|)$ . For our specific examples where we fixed  $\lambda^2 = 0.1$ , we predict  $S_0 \sim 0.8$ .

## Acknowledgments

The authors wish to thank Jorge Russo for discussions, and Roberto Emparan for comments on the first draft of the paper. MK is supported by the Joan Oró fellowship. Our research is financed by the grant PID2022-136224NB-C22, funded by MCIN/AEI/10.13039/501100011033/FEDER, UE, by the grant 2021-SGR00872 and CEX2024-001451-M funded by MICIU/AEI/10.13039/501100011033.

## References

- [1] S.W. Hawking, *Black hole explosions*, *Nature* **248** (1974) 30.
- [2] S.W. Hawking, *Particle Creation by Black Holes*, *Commun. Math. Phys.* **43** (1975) 199.
- [3] S.W. Hawking, *Breakdown of Predictability in Gravitational Collapse*, *Phys. Rev. D* **14** (1976) 2460.
- [4] D.N. Page, *Information in black hole radiation*, *Physical Review Letters* **71** (1993) 3743–3746.



- [5] D.N. Page, *Average entropy of a subsystem*, *Physical Review Letters* **71** (1993) 1291–1294.
- [6] R. Jackiw, *Lower Dimensional Gravity*, *Nucl. Phys. B* **252** (1985) 343.
- [7] C. Teitelboim, *Gravitation and Hamiltonian Structure in Two Space-Time Dimensions*, *Phys. Lett. B* **126** (1983) 41.
- [8] J. Maldacena, D. Stanford and Z. Yang, *Conformal symmetry and its breaking in two dimensional Nearly Anti-de-Sitter space*, *PTEP* **2016** (2016) 12C104 [[1606.01857](#)].
- [9] A. Almheiri and J. Polchinski, *Models of  $AdS_2$  backreaction and holography*, *JHEP* **11** (2015) 014 [[1402.6334](#)].
- [10] J. Engelsöy, T.G. Mertens and H. Verlinde, *An investigation of  $AdS_2$  backreaction and holography*, *JHEP* **07** (2016) 139 [[1606.03438](#)].
- [11] S. Sachdev, *Holographic metals and the fractionalized Fermi liquid*, *Phys. Rev. Lett.* **105** (2010) 151602 [[1006.3794](#)].
- [12] J.S. Cotler, G. Gur-Ari, M. Hanada, J. Polchinski, P. Saad, S.H. Shenker et al., *Black Holes and Random Matrices*, *JHEP* **05** (2017) 118 [[1611.04650](#)].
- [13] J. Maldacena and D. Stanford, *Remarks on the Sachdev-Ye-Kitaev model*, *Phys. Rev. D* **94** (2016) 106002 [[1604.07818](#)].
- [14] P. Saad, S.H. Shenker and D. Stanford, *A semiclassical ramp in SYK and in gravity*, [1806.06840](#).
- [15] F. Haake, *Quantum Signatures of Chaos*, Springer Series in Synergetics, Springer, Berlin (2010), [10.1007/978-3-642-05428-0](#).
- [16] P. Saad, S.H. Shenker and D. Stanford, *JT gravity as a matrix integral*, [1903.11115](#).
- [17] P. Saad, *Late Time Correlation Functions, Baby Universes, and ETH in JT Gravity*, [1910.10311](#).
- [18] D. Stanford and E. Witten, *JT gravity and the ensembles of random matrix theory*, *Adv. Theor. Math. Phys.* **24** (2020) 1475 [[1907.03363](#)].
- [19] T.G. Mertens and G.J. Turiaci, *Solvable models of quantum black holes: a review on Jackiw–Teitelboim gravity*, *Living Rev. Rel.* **26** (2023) 4 [[2210.10846](#)].
- [20] A. Blommaert, T.G. Mertens and H. Verschelde, *Clocks and Rods in Jackiw-Teitelboim Quantum Gravity*, *JHEP* **09** (2019) 060 [[1902.11194](#)].
- [21] D. Marolf and H. Maxfield, *Transcending the ensemble: baby universes, spacetime wormholes, and the order and disorder of black hole information*, *JHEP* **08** (2020) 044 [[2002.08950](#)].
- [22] P. Saad, S.H. Shenker, D. Stanford and S. Yao, *Wormholes without averaging*, *JHEP* **09** (2024) 133 [[2103.16754](#)].
- [23] C. Germani, *Retrieving black hole information from the main Lorentzian saddle point*, *Phys. Rev. D* **106** (2022) 066018 [[2204.13046](#)].
- [24] M. Spradlin and A. Strominger, *Vacuum states for  $AdS(2)$  black holes*, *JHEP* **11** (1999) 021 [[hep-th/9904143](#)].
- [25] U.H. Danielsson, E. Keski-Vakkuri and M. Kruczenski, *Vacua, propagators, and holographic probes in  $AdS / CFT$* , *JHEP* **01** (1999) 002 [[hep-th/9812007](#)].
- [26] W.G. Unruh, *Notes on black hole evaporation*, *Phys. Rev. D* **14** (1976) 870.

- [27] J.M. Maldacena, *Eternal black holes in anti-de Sitter*, *JHEP* **04** (2003) 021 [[hep-th/0106112](#)].
- [28] J. Maldacena and L. Susskind, *Cool horizons for entangled black holes*, *Fortsch. Phys.* **61** (2013) 781 [[1306.0533](#)].
- [29] S. Ryu and T. Takayanagi, *Aspects of Holographic Entanglement Entropy*, *JHEP* **08** (2006) 045 [[hep-th/0605073](#)].
- [30] D. Stanford and E. Witten, *Fermionic Localization of the Schwarzian Theory*, *JHEP* **10** (2017) 008 [[1703.04612](#)].
- [31] Y.-H. Qi, Y. Seo, S.-J. Sin and G. Song, *Correlation functions in Schwarzian liquid*, *Phys. Rev. D* **99** (2019) 066001 [[1804.06164](#)].
- [32] Y.-H. Qi, Y. Seo, S.-J. Sin and G. Song, *Correlation functions in Schwarzian liquid*, *Phys. Rev. D* **99** (2019) 066001 [[1804.06164](#)].
- [33] E. Witten, *Anti de Sitter space and holography*, *Adv. Theor. Math. Phys.* **2** (1998) 253 [[hep-th/9802150](#)].